Target Classification with Low-Resolution Radars Based on Multifractal Features in Fractional Fourier Domain

Huaxia Zhang, Qiusheng Li, Chuicai Rong, and Xindi Yuan[*]

Abstract—Due to the limitations of low-resolution radar system and background clutter, the task of target classification with conventional low-resolution radars is relatively difficult. This paper introduces fractional Fourier transform (FrFT) to process aircraft echoes in order to find the optimal fractional Fourier domain, in which signal to noise ratio can reach the maximum, and then applies multifractal theory to the feature extraction of radar targets. Based on the above, we use SVM to do target classification. Experiments show that the multifractal characteristics of aircraft echoes can be enhanced by FrFT, and the features extracted from the optimal fractional Fourier domain can be used effectively to classify different types of aircraft even in the case of low SNR.

1. INTRODUCTION

Most surveillance radars adopt conventional low-resolution radar systems, which are mainly used for target detection and tracking. Surveillance radars have been restricted in the application of target classification in consequence of the limitations of conventional low-resolution radar system. For instance, single-polarization narrow-band transmitting signals cannot fully stimulate the physical characteristics of aircraft easily, low pulse repetition frequency and short irritation time [1, 2]. The features that can be used to identify aircraft targets with low-resolution radars can be divided into three categories: fluctuation characteristics of aircraft echoes (radar cross-section (RCS), fluctuation of amplitude and phase, two-dimensional gray scale, etc.), motion characteristics of aircraft (height, speed and acceleration, etc.) and jet engine modulation (JEM) features. Considering all feature extraction methods, the way based on JEM features accounts for a large proportion [3–9]. Fractional Fourier transform (FrFT) is a generalized form of Fourier transform (FT), which combines the information both from time domain and frequency domain. Based on the existing feature extraction methods, Du et al. introduced FrFT to extract the features of jet aircraft, propeller aircraft and helicopters, and then combined with linear relevance vector machine to classify the three types of aircraft [10]. Yu et al. used FrFT to do detection and delay estimation of moving targets in strong clutter background [11]. Elgamel and Soraghan, adapted FrFT to do adaptive filtering of radar data [12]. Radar target echoes, background and sea clutter of radars all have multifractal characteristics [13–15]. On the basis of fractal determination and non-scaling interval estimation, Li et al. analyzed multifractal characteristics of conventional low-resolution radars by applying fractal theory [16–18]. The above researches show that FrFT and fractal analysis can effectively enhance the classification rates of conventional low-resolution radars.

In this paper, we use FrFT to dispose low-resolution radar echoes and analyze their multifractal characteristics in the optimal fractional Fourier domain, and discuss the classification performance of different types of low-resolution radars combining with SVM. Firstly, we introduce the theoretical basis of fractional Fourier transform and multifractal. Then, we analyze the multifractal characteristics of

* Corresponding author: Xindi Yuan (yxdi@yeah.net).
The authors are with the School of Physics and Electronic Information, Gannan Normal University, Ganzhou 341000, China.

the measured low resolution radar echoes in the optimal fractional Fourier domain and further extract the multifractal features in order to do target classification. Lastly, we verify the classification and recognition performance of the algorithm by means of measured radar echoes data.

2. THEORETICAL ANALYSIS

2.1. Fractional Fourier Transform (FrFT)

FrFT is the generalized form of Fourier transform (FT). On the one hand, it reserves the superiorities of FT; on the other hand, it has many special properties. FrFT can be viewed as a ray that transforms the signal from the time axis to u axis by rotating the angle α counterclockwise. The pth order FrFT of the signal $f(t)$ can be defined as follows:

$$f_p(u) = \int_{-\infty}^{\infty} K_p(u,t)f(t)dt \tag{1}$$

$$k_p(t,u) = \begin{cases} A_a \exp\left[j\pi\left(u^2\cot\alpha - 2u\csc\alpha + t^2\cot\alpha\right)\right], & a \neq n\pi \\ \delta(t-u), & \alpha = 2n\pi \\ \delta(t-u), & \alpha = (2n+1)\pi \end{cases} \tag{2}$$

$f_p(u)$ is the signal obtained by the pth order of FrFT in fractional Fourier domain, and $K_p(u,t)$ is the kernel function of FrFT, where $A_a = \sqrt{1 - j\cot\alpha}$, $\alpha = p\pi/2$, $p \neq 2n$, $n \in Z$. Actually, in digital signal processing, we generally need the discrete form of FrFT, and this paper uses the method that transforms FrFT into the convolution form to obtain the discrete form of FrFT [11, 19].

By using the Shannon interpolation formula:

$$f_p(u) = \sqrt{\frac{1 - j\cot\alpha}{2\pi}}\exp\left(j\pi u^2\cot\alpha\right) \times \int_{-\infty}^{\infty}\left[f(t)\exp\left(j\pi t^2\cot\alpha\right) \times \exp\left(-j2\pi tu\csc\alpha\right)\right]dt \tag{3}$$

$$f(t)\exp\left(j\pi t^2\cot\alpha\right) = \sum_{n=-N}^{N} f\left(\frac{n}{2\Delta x}\right)\exp\left[\frac{j\pi\cot\alpha n^2}{(2\Delta x)^2}\right] \times \sin c\left[2\Delta x\left(t - \frac{n}{2\Delta x}\right)\right] \tag{4}$$

Substitute Eq. (4) into Eq. (3), we can yield the discrete form of FrFT:

$$\begin{aligned} f_p\left(\frac{m}{2\Delta x}\right) &= \frac{A_a}{2\Delta x}\exp\left\{\frac{j\pi\left[\cot\alpha - \csc\alpha\right]m^2}{(2\Delta x)^2}\right\} \times \sum_{n=-N}^{N}\exp\left[\frac{j\pi(\cot\alpha)(m-n)^2}{(2\Delta x)^2}\right] \\ &\times \exp\left\{\frac{j\pi\left[\cot\alpha - \csc\alpha\right]n^2}{(2\Delta x)^2}\right\} f\left(\frac{n}{2\Delta x}\right), \end{aligned} \tag{5}$$

where $1/\Delta x$ is the sampling interval of the time domain; n and m are the sampling points of time domain and fractional Fourier domain respectively; N denotes the total number of time domain samples. If $f(t)$ is a linear frequency modulation signal, its FrFT $f_p(m/2\Delta x)$ forms an impulse function in the optimal fractional Fourier domain, so that the energy can be maximally aggregated.

2.2. Multifractal Analysis

What multifractal theory describes is the characteristics of different levels of a factual object during the growth process. The investigated object can be divided into many small regions, whose total number is N, and ε is the size ($\varepsilon < 1$) of a small region. The growth probability of the ith small region is $P_i(\varepsilon)$, and σ_i indicates the growth probabilities of different regions. The relationship between $P_i(\varepsilon)$ and ε is:

$$p_i(\varepsilon) \propto \varepsilon^{\sigma_i}, \quad i = 1, 2, \cdots, N \tag{6}$$

where σ_i can be called local fractal dimension (LFD) or singular index, whose value reflects the size of growth probability of fractal in a small region. If different regions have different singular indexes, the fractal is a multifractal geometry; if all singular indexes are almost the same, the fractal can almost be

considered as a monofractal geometry. Eq. (6) takes the power of q and sums to obtain the partition function:

$$\Gamma(q,\varepsilon) = \sum_{i=1}^{N} P_i^q(\varepsilon) = \varepsilon^{\tau(q)} \propto \sum_{i=1}^{N} \varepsilon^{\sigma_i q}, \quad q \in (-\infty, +\infty) \tag{7}$$

In Eq. (7), if $q \gg 1$, the subsets with large probabilities dominate; if $q \ll 1$, the subsets with small probabilities play a major role. In practical application, the range of q can be determined according to specific conditions. We can see from Eq. (7) that the partition function $\Gamma(q,\varepsilon)$ and ε have power-law relationship, and their slope, denoted as $\tau(q)$, is called the mass index. If $\tau(q)$ is a linear function of q, the fractal has monofractal properties; if $\tau(q)$ is a convex function of q, the fractal has multifractal characteristics.

The definition of multifractal spectrum $f(\sigma)$ is the fractal dimension of fractal subset with the same singular index. We can use the infinite sequences of $f(\sigma)$, corresponding to different σ, to represent the fractal dimension of the entire fractal in order to reflect the characteristics of the growth distribution probability. In [19], it has been proved that $\tau(q)$, q and $f(\sigma)$, σ have the relationship of Legendre transform, so the multifractal spectrum $f(\sigma)$ can be obtained by the Legendre transform of mass index $\tau(q)$.

3. THE MULTIFRACTAL FEATURE EXTRACTION METHOD

During the short time when an aircraft is being exposed to the irradiation of the radar, the target can be viewed as a dot moving with a uniform acceleration. To simplify the description, the target classification method is based on multifractal features in fractional Fourier domain (MFIFFD). Next we study the implementation steps and classification performance of MFIFFD algorithm.

3.1. Determination of the Optimal Fractional Fourier Domain

In the optimal fractional Fourier domain, the energy of the aircraft echoes can be maximally aggregated, and the distribution of clutter is relatively dispersed, so we should find the optimal fractional Fourier domain of low-resolution radar echoes. Before feature extraction, we take FrFT to process the aircraft echoes and further confirm the optimal fractional Fourier order. In information theory, entropy can represent the average information of a signal and reflect the degree of distribution of echo energy. Renyi entropy is a generalized form of Shannon entropy, which has more generality in measuring the information. Third-order Renyi information entropy is an effective tool for measuring the information of time-frequency distribution. The maximum value of the third-order Renyi information entropy indicates that the time-frequency distribution of the analyzed signal has the highest aggregation [20]. Refs. [21, 22] use third-order Renyi information entropy to measure the time-frequency aggregation of the observed signal. In the paper, we also use third-order Renyi information entropy to measure the aggregation performance of aircraft echoes in time-frequency domain. We do feature extraction of aircraft echoes in the optimal fractional Fourier domain later. It is considered that the fractional Fourier domain, whose transform order is the optimal transform order p_{opr}, is the optimal fractional Fourier domain.

The optimal transform order p_{opr} corresponds to the maximum value of the third-order Renyi information entropy.

The definition of third-order Renyi information entropy:

$$v = -1/2 \sum_k \log\left(|\mathrm{FrFT}_P(K)|^3\right) \tag{8}$$

Different types of aircraft have different structural parameters, and their third-order Renyi information entropies are also different. As for the same aircraft, the third-order Renyi information entropy can also be influenced by the speed, acceleration, altitude, environment, etc. Different third-order Renyi information entropies generally have different optimal transform orders of FrFT, so every experiment needs to determine the optimal transform order of FrFT in order to achieve specific analysis of specific experiment. In order to verify the effectiveness of the algorithm, we use the measured radar echoes to carry out the following experiments. In experiment, we select six kinds of aircraft, three of which were to fly toward the station and three to fly off the station. The radar worked in the VHF band with pulse
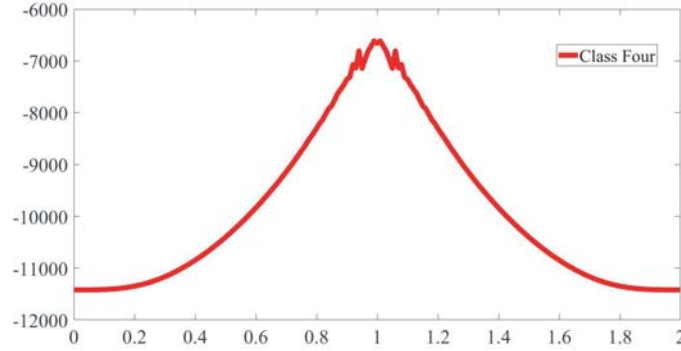
Figure 1. The third-order Renyi information entropy curve of jet aircraft.

repetition frequency of 100 Hz and pulse width of 25 μs. Calculating the third-order Renyi information entropies of six types of aircraft respectively with the range [0, 2] and the step of transform order p 0.01, respectively, we can obtain their optimal transform orders of FrFT and further determine their optimal fractional Fourier domains. In Fig. 1, we chose one of the six types of aircraft, the fourth class, to plot the third-order Renyi information entropy of target echoes. For other types of aircraft, the third-order Renyi information entropy curves are roughly similar.

3.2. Extraction of Multifractal Features

By using FrFT to process the original aircraft echoes and further determining the optimal transform orders, we can do multifractal analysis of radar echoes in the optimal fractional Fourier domain. Fractal theory is based on the fractals which have self-similarity and should be studied in the non-scale interval, so it is necessary to further discuss whether the radar echoes have multifractal characteristics in the optimal fractional Fourier domain. There are six types of aircraft targets, and the radar working parameters have been described above. We compare the multifractal characteristics of six kinds of aircraft in time domain and the optimal fractional Fourier domain. The experimental results are shown in Figs. 2 ∼ 5.

As can be seen from Fig. 2(a) and Fig. 3(a), the mass index curves of six kinds of aircraft are approximately linear, that is to say, the multifractal characteristics of aircraft echoes in time domain are inconspicuous. After using FrFT to process the aircraft echoes, their multifractal characteristics can be enhanced evidently as shown in Fig. 2(b) and Fig. 3(b), and the relationship between q and $\tau(q)$ is obvious convex functions.
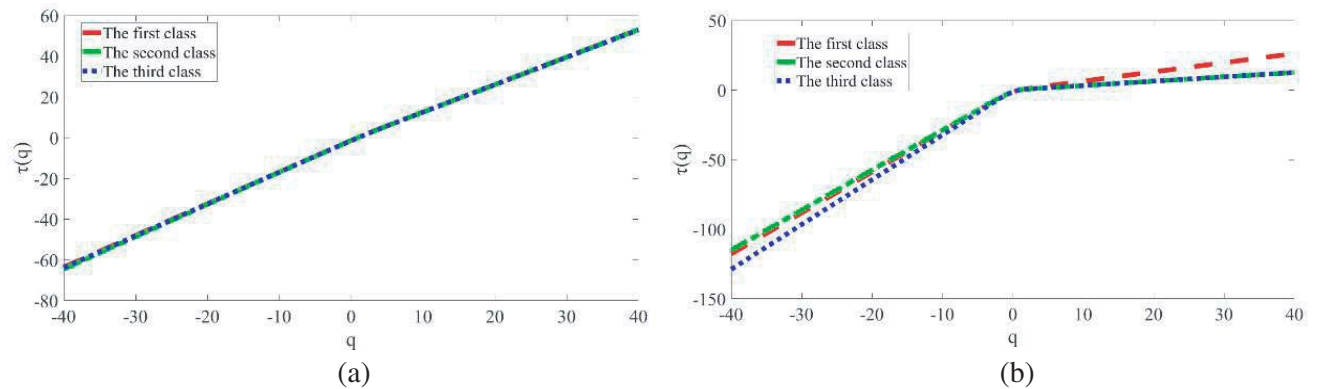

(a)

(b)

Figure 2. The mass index curves of three types of aircraft flying toward the station. (a) Not doing FrFT. (b) Doing FrFT.

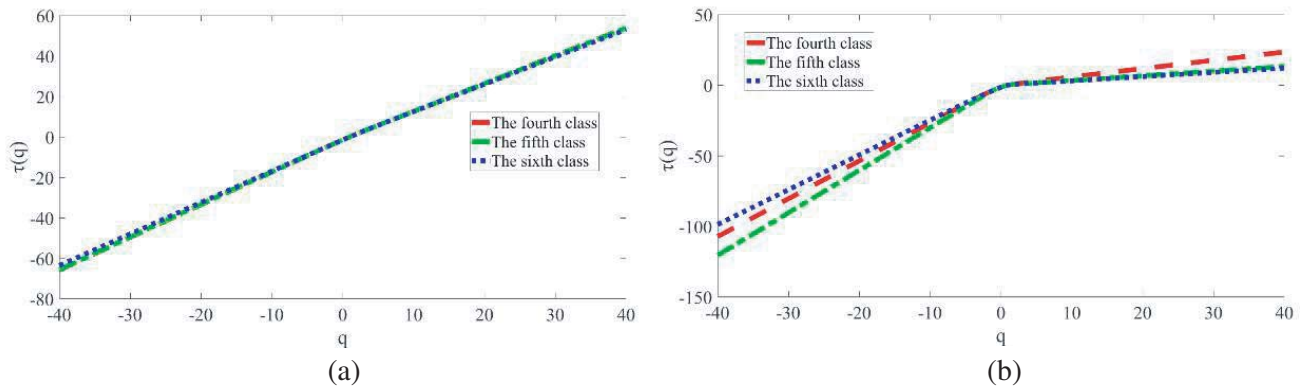(a)   (b)

Figure 3. The mass index curves of three types of aircraft flying off the station. (a) Not doing FrFT. (b) Doing FrFT.

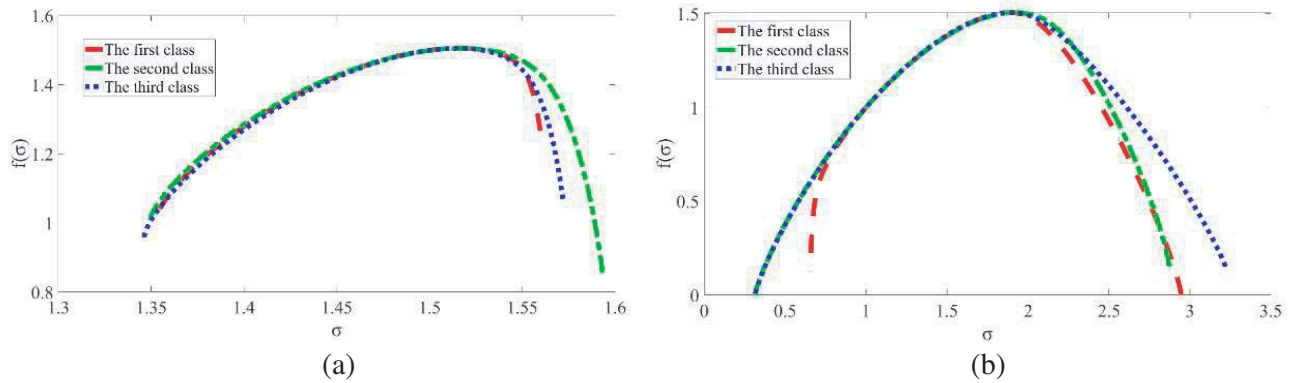(a)   (b)

Figure 4. The multifractal spectrum of three types of aircraft flying toward the station. (a) Not doing FrFT. (b) Doing FrFT.

(a)   (b)
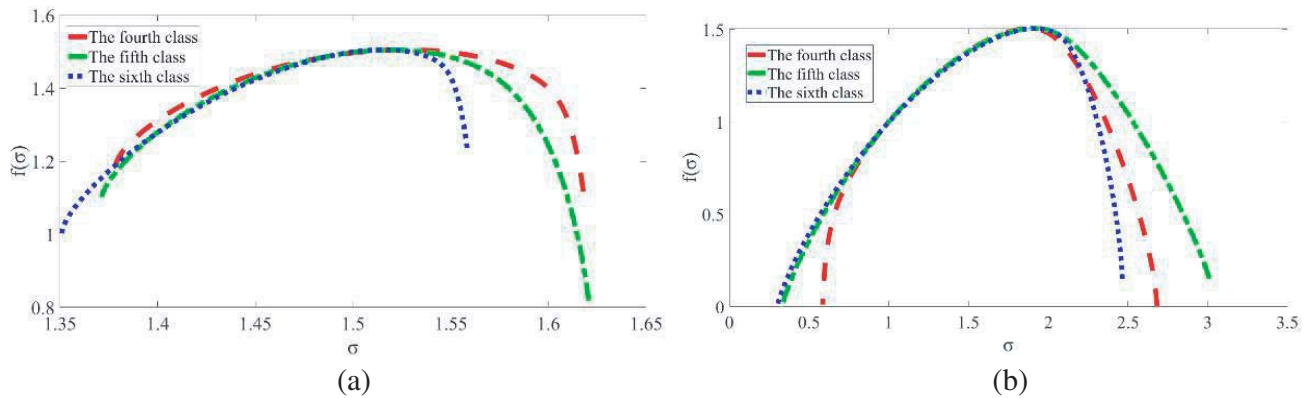
Figure 5. The multifractal spectrum of three types of aircraft flying off the station. (a) Not doing FrFT. (b) Doing FrFT.

It can be seen from Fig. 4(a) and Fig. 5(a) that the distribution ranges of the six types of aircraft are relatively narrow, which verifies the approximately linear relationship of the mass index curves in Fig. 2(a) and Fig. 3(a). After FrFT, we can conclude from Fig. 4(b) and Fig. 5(b) that the distribution ranges of singular index σ of all types of aircraft have been significantly increased. For the first three types of aircraft, the range of singular index σ of the third class increased the most, followed by the

second class. For the last three types of aircraft, the range of singular index σ of the fifth class increased the most, followed by the sixth class. Compared with the aircraft flying off the station, the multifractal characteristic of the aircraft in the case of flying toward the station is more obvious.

The experiments verify that the aircraft echoes have multifractal characteristics in the optimal fractional Fourier domain, and their properties can be enhanced by FrFT. From Figs. $2 \sim 5$, we can see that the shapes of multifractal spectrums $f(\sigma)$ and mass index curves $\tau(q)$ are obviously different, so we can extract the differences of multifractal curves as feature vectors to discriminate six types of aircraft targets. We use the following three multifractal characteristic parameters to classify the aircraft:

(1) The difference of fractal dimension between the maximum probability and minimum probability subset

$$\Delta f = |f(\sigma_{\max} - \sigma_{\min})| \tag{9}$$

where $\sigma_{\max}$ represents the maximum singular index σ, corresponding to the minimum probability subset, and $\sigma_{\min}$ denotes the minimum singular index σ, corresponding to the maximum probability subset.

(2) Multifractal spectral width $\Delta\sigma$

$$\Delta\sigma = \sigma_{\max} - \sigma_{\min} \tag{10}$$

(3) Mass index symmetry R_τ

$$R_\tau = \left| \frac{\max(\tau(q))}{\min(\tau(q))} \right| \tag{11}$$

Figs. $6 \sim 7$ show the probability density distribution of the three multifractal parameters of six types of aircraft echoes. The working conditions and parameters of radar have been shown above. In the case of an aircraft flying toward the station, three multifractal characteristics all have strong ability
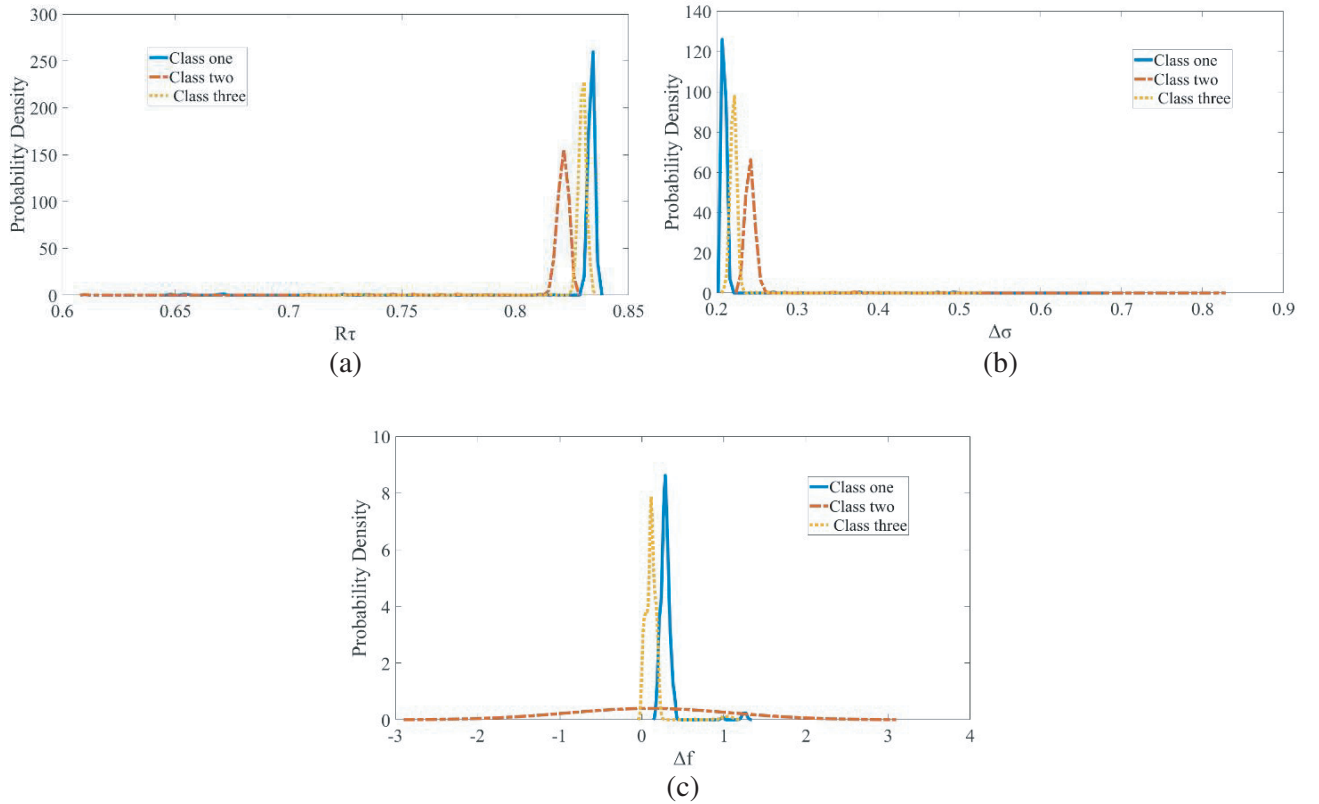

Figure 6. Probability density distributions of multifractal features of aircraft flying toward the station. (a) Mass index symmetry $R\tau$. (b) Multifractal spectral width $\Delta\sigma$. (c) The difference of fractal dimension Δf.
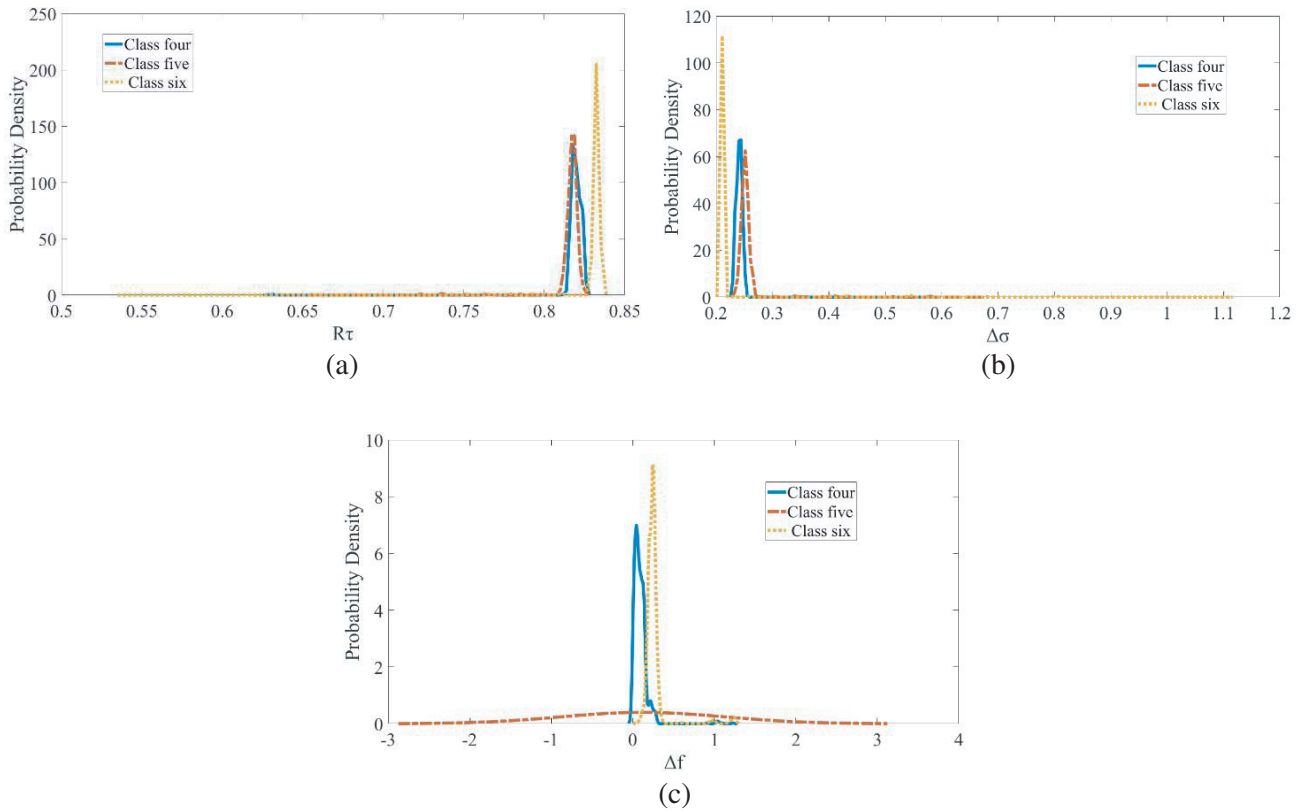
Figure 7. Probability density distributions of multifractal features of aircraft flying off the station. (a) Mass index symmetry $R\tau$. (b) Multifractal spectral width $\Delta\sigma$. (c) The difference of fractal dimension Δf.

for target classification. In the case of an aircraft flying off the station, the sixth type of aircraft can be easily separated from the three kinds of aircraft, and the difference of fractal dimension between the maximum probability and minimum probability subset can easily distinguish the three types of radars. Intuitively, although the multifractal characteristics overlapped within a certain range, it is hopeful to get a better performance by comprehensive utilization of the three features.

4. CLASSIFICATION EXPERIMENTS

In this part, we experimentally study the performance of MFIFFD method for aircraft target classification and recognition with the measured data. In [18], it has been proved that the radar target correct classification rate (CCR) based on multifractal features in time domain is higher than that of dispersion situations of eigenvalue spectra. In [1], it has been confirmed that the target classification performance of extended fractal features was superior to that of characteristic spectrum and fractional Brownian method. To simplify the description, the classification method described in [18] is called MFITD, and the method proposed in [1] is called EFITD in the following text. MFITD extracts the multifractal characteristics in time domain; EFITD reveals the extended fractal features also in time domain; MFIFFD analyses the multifractal characteristics in the optimal fractional Fourier domain. MFITD extracts the multifractal characteristics in time domain, and MFIFFD analyses the multifractal characteristics in the optimal fractional Fourier domain. We compare the classification and recognition performance among MFIFFD, EFIFFD, and MFITD using the measured aircraft and radar data that have been shown in the above experiments.

SVM has the superiorities of strong generalization ability and fast convergence speed, so the experiments utilize SVM as a classifier to compare the classification performance between MFIFFD

and MFITD. The SVM classifier adopts Gaussian kernel function $K(x_i, x_j) = \exp(-\|x_i - x_j\|^2 / \sigma^2)$. As we all know, there is no prior knowledge about parameter σ^2, and in the following experiments, we will try different values many times without going beyond the calculation burden to get the reasonable parameters. In this way, the simulation results can obtain better CCRs under the reasonable selection of parameters of Gaussian kernel function.

    Experiment 1: In order to verify the effectiveness of the algorithm, we use the measured radar echoes to carry out the following experiments. The radar worked in the in VHF band with pulse repetition frequency of 100 Hz and pulse width of 25 μ. There are six kinds of aircraft, and each type of aircraft collects 1024 sets of echoes, of which 512 sets of data are used as training data and 512 sets of data used for testing data. Table 1 shows the CCRs of MFIFFD and MFITD in the condition of aircraft flying toward the station. Table 2 shows the CCRs of MFIFFD and MFITD in the condition of aircraft flying off the station.

Table 1. CCRs of MFIFFD and MFITD.

Comparative Items	MFITD		EFITD		MFIFFD	
	Training Data	Testing Data	Training Data	Testing Data	Training Data	Testing Data
The first class/%	97.02	96.24	100	98.55	99.61	99.61
The second class/%	90.99	89.54	100	100	98.84	98.65
The third class/%	93.50	90.76	100	98.75	100	99.80
Average CCRs/%	92.85	94.50	100	99.10	99.48	99.35

Table 2. CCRs of MFIFFD and MFITD.

Comparative Items	MFITD		EFITD		MFIFFD	
	Training Data	Testing Data	Training Data	Testing Data	Training Data	Testing Data
The fourth class/%	93.37	93.28	100	100	96.75	96.65
The fifth class/%	86.46	82.86	100	97.94	98.21	95.18
The sixth class/%	93.32	92.65	100	91.69	100	99.61
Average CCRs/%	91.05	89.60	100	96.39	98.32	97.15

    We can see, from both Table 1 and Table 2, that for all the six kinds of aircraft, the CCRs and average CCRs of MFIFFD are higher than MFITD, and MFIFFD can achieve better classification performance. The average CCRs of training data of EFITD are higher than that of MFIFFD, but the average CCRs of testing data of EFITD are lower than that of MFIFFD. As for the MFIFFD method, in the case of toward-station situation, the CCR of the third kind of aircraft is the highest, followed by the first type of aircraft. In the off-station situation, the CCR of the sixth type of aircraft is the highest, followed by the fourth type of aircraft. The CCRs of aircraft flying toward the station is superior to CCRs of aircraft flying off the station.

    Experiment 2: In this experiment, we further investigate the classification and recognition performance of multifractal features of MFIFFD method under low SNRs (signal to noise ratio), and the measured radar echoes are described above. We take the first three kinds of aircraft, and the aircraft flied toward the station as an example. We add Gauss white noise with different intensities to the measured target echoes. We also use SVM as a classifier to do radar target classification. Table 3 shows average CCRs of the first three kinds of aircraft under different SNRs. It can be seen from Table 3 that the multifractal features have strong robustness, and even under the condition of −5 dB SNR, the average CCR of aircraft can still reach more than 92%. This experiment demonstrates the effectiveness of the extracted features and the feasibility of the MFIFFD method.

Table 3. Classification and identification results under different SNRs.

SNR/dB	2	0	−0.5	−1	−2	−5
Average CCRs/%	99.48	99.35	98.61	94.86	92.48	92.37

Compared with MFITD, the multifractal characteristics of MFIFFD are calculated in the optimal fractional Fourier domain, so MFIFFD had to carry out the calculation of third-order Renyi information entropy and fractional Fourier transform. In the above experiments, we have six types of aircraft, each of which has 1024 sets of echoes, and the length of each set of echo data is 1024. The running time of the algorithm can illustrate the complexity of the algorithm to a certain extent. Although the running time of MFIFFD is 174.163 seconds more than MFITD, 139.21 seconds, the computational complexity of MFIFFD is still within the allowable range due to the huge data of radar echoes. EFITD and MFIFFD have similar classification performances, but the classification features of EFITD are generalized Hurst exponents without any dimensionality reduction. Compared with MFIFFD, EFITD has higher feature dimension and longer classification and recognition time.

5. CONCLUSIONS

In this paper, we have proposed a new method by using FrFT and multifractal theory to do low-resolution radar target classification. We firstly use the third-order Renyi information entropy to calculate the optimal transform orders in order to determine the optimal transform Fourier domains of FrFT and then adopt the multifractal theory to extract the multifractal features for target classification. Experimental results show that not only the low-resolution radar echoes have multifractal characteristics, but also their features can be enhanced by FrFT. The average CCRs of MFIFFD are higher than that of MFITD, and the CCRs of aircraft in the case of toward the station are higher than that off the station. Although the computational complexity of the third-order Renyi entropy is very small, it also increases the complexity of the algorithm to some extent. In view of the limitations of low-resolution radar system, it is only applicable to the rough target classification of conventional radars, although the CCRs have been greatly improved.

ACKNOWLEDGMENT

REFERENCES

1. Li, Q. S., W. X. Xie, and J. X. Huang, "Extended fractal characteristic analysis and target classification study of surveillance radar echoes," *Journal of Signal Processing*, Vol. 29, No. 9, 1091–1097, 2013.
2. Yong, Y. W., P. J. Hoon, B. J. Wu, et al., "Automatic feature extraction from jet engine modulation signals based on an image processing method," *IET Radar, Sonar & Navigation*, Vol. 9, No. 7, 783–789, 2015.
3. Yang, S. F., H. K. Wu, X. Wang, et al., "Target feature extraction and recognition based on low-resolution radar," *Electronic Information Countermeasures Technology*, Vol. 30, No. 4, 15–20, 2015.
4. Zhang, G. W., R. Li, and D. Wang, "An overview of low resolution radar target classification methods," *Digital Communication World*, Vol. 5, 280, 2018.

5. Huang, P. K., H. C. Yin, and X. J. Xu, *Radar Target Characteristics*, 114–115, Beijing Electronic Industry Press, 2005.

6. Yun, S., H. L. Wang, H. J. Zhang, et al., "Target recognition of low resolution radar based on waveform feature," *Shipboard Electronic Countermeasure*, Vol. 38, No. 4, 62–69, 2015.

7. Chen, H., Y. Ding, X. H. Jiao, et al., "Target recognition for low resolution radar based on generalized fuzzy function," *Shipboard Electronic Countermeasure*, Vol. 39, No. 5, 46–49, 2016.

8. Song, X. J., "Research on target classification and identification of low-resolution radar," *Radar Science and Technology*, Vol. 14, No. 3, 286–290, 2016.

9. Li, Q., H. Zhang, Q. Lu, and L. Wei, "Research on analysis of aircraft echo characteristics and classification of targets in low-resolution radars based on EEMD," *Progress In Electromagnetics Research M*, Vol. 68, 61–68, 2018.

10. Du, L., H. R. Shi, L. S. Li, et al., "Feature extraction method for target echo of narrowband radar aircraft based on fractional Fourier transform," *Journal of Electronics and Information*, Vol. 38, No. 12, 3093–3099, 2016.

11. Yu, G., S. C. Piao, and X. Han, "Fractional Fourier transform-based detection and delay time estimation of moving target in strong reverberation environment," *IET Radar, Sonar & Navigation*, Vol. 11, No. 9, 1367–1372, 2017.

12. Elgamel, S. A. and J. Soraghan, "A new fractional Fourier transform based monopulse tracking radar processor," *2010 IEEE International Conference on Acoustics, Speech, and Signal Processing, ICASSP 2010 — Proceedings*, Institute of Electrical and Electronics Engineers Inc., 2010.

13. Xian, M., Z. W. Zhuang, S. P. Xiao, et al., "Chaotic multifractal analysis and identification of radar target echoes," *Journal of National University of Defense Technology*, Vol. 2, 63–67, 1998.

14. Shi, Z. G., J. X. Zhou, H. Z. Zhao, et al., "Multifractal analysis of sea clutter," *Data Acquisition and Processing*, Vol. 2, 168–173, 2006.

15. Li, Q. S., X. Y. Liu, and J. P. Chen, "Research on fractal modeling of aircraft echoes and classification of targets in conventional radars," *Journal of Gannan Normal University*, Vol. 36, No. 3, 34–39, 2015.

16. Li, Q. S., X. D. Yuan, and L. X. Guan, "Analysis of the multifractal characteristics of the conventional radar return signal from aircraft targets," *Journal of Anhui University (Natural Science Edition)*, Vol. 36, No. 5, 47–54, 2012.

17. Li, Q. S. and W. X. Xie, "Target classification with low-resolution surveillance radars based on multifractal features," *Computer Application Research*, Vol. 30, No. 2, 405–409, 2013.

18. Li, Q. S., X. C. Xie, H. Zhu, et al., "Fractal characteristic analysis and target classification of aircraft echoes of low-resolution radars in fractional Fourier domain," *Application Research of Computers*, Vol. 35, No. 9, 2869–2872, 2018.

19. Ozaktas, H. M., O. Arikan, M. A. Kutay, et al., "Digital computation of the fractional Fourier transform," *IEEE Transactions on Signal Processing*, Vol. 44, No. 9, 2141–2150, 1996

20. Williams, W. J., "Uncertainty, information, and time-frequency distributions," *Proceedings of SPIE, The International Society for Optical Engineering*, Vol. 1566, 144–156, 1991.

21. Hao, B. and M. Luo, "Performance analysis and interference suppression method of GPS system under time-varying single-tone interference," *Computer Application Research*, Vol. 35, No. 321(7), 185–188, 2018.

22. Ouyang, X. and M. G. Amin, "Short-time Fourier transform receiver for nonstationary interference excision in direct sequence spread spectrum communications," *IEEE Transactions on Signal Processing*, Vol. 49, No. 4, 851–863, 2001.